Macromolecules

ARTICLE

pubs.acs.org/Macromolecules

New Approach for the Elucidation of PCM Nanocapsules through Miniemulsion Polymerization with an Acrylic Shell

Abbas Rezaee Shirin-Abadi,[†] Ali Reza Mahdavian,[*,‡] and Sepideh Khoee[†]

[†]Polymer Laboratory, Chemistry Department, School of Science, University of Tehran, P.O. Box 14155-6455, Tehran, Iran

[‡]Polymer Science Department, Iran Polymer & Petrochemical Institute, P.O. Box 14965-115, Tehran, Iran

ABSTRACT: The aim of this study is to investigate the in situ encapsulation of *n*-hexadecane as a phase change material (PCM) with a polymethyl methacrylate (PMMA) shell through miniemulsion polymerization. *n*-Hexadecane (HD) and methyl methacrylate (MMA) form dispersed minidroplets in the aqueous phase, whereas PMMA is immiscible with *n*-hexadecane and separates through polymerization to produce hollow polymer particles filled with *n*-hexadecane. Different HD:MMA ratios and ethylene glycol dimethacrylate (EGDMA) as a cross-linking agent were considered to optimize the encapsulation process. A new approach by using novel equations from DSC, DLS, and microscopy analyses were developed to estimate shell thickness and the extent of contribution of MMA in the formation of the nanocapsules, pure polymeric particles, and also the void fraction of nanocapsules. It was found that the weight fractions of pure polymeric particles for the prepared samples were 12−17 wt %, and the shell thickness of the nanocapsules was about 12 nm. Also, the void fractions for these samples were 69−77%.

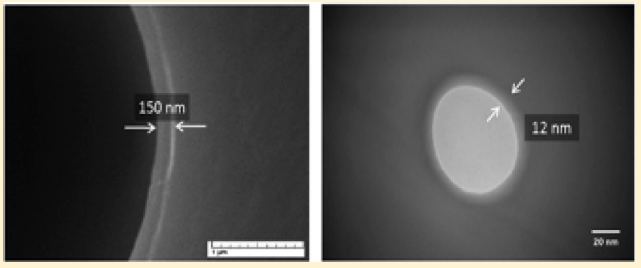

INTRODUCTION

The research on nano/microencapsulation emerged in the 1950s and was rapidly expanded in the 1970s, originally directing toward entrapping solids, liquids, or gases into polymeric shells. Today, nano/microcapsules have been developed, studied, and used by scientists and engineers of different backgrounds throughout the chemistry and life sciences, biotechnology, medicine, and related industries because of the many advantages afforded by these encapsulated systems. A wide range of core materials have been encapsulated, including adhesives, drugs, agricultural aids, paper coating, enzymes, salts, dyes, electronic ink, fragrant oils, long chain normal alkanes, waxes, etc.[1−6] Among them, encapsulation of paraffin and waxes as PCMs is one of the most important research as well as industrial applications because according to the growing energy crisis, there are more and more research interests on renewable energy sources and materials through out the world.[7,8] Therefore, thermal energy storage from clean sources is considered as one of the advanced energy technologies.[9,10] As renewable and clean energy storage materials, PCMs have been employed in many fields, based on their properties. PCMs with their high-energy storage density and small temperature variation from storage to retrieval have been studied for several decades and applied as solar energy storage,[11] thermal storage building materials,[12] air conditioning,[13] thermo-regulating, or intelligent textiles.[14] Since PCMs melt and crystallize repeatedly during use, there is a risk of PCM leakage; additionally, low conductivity and tendency for supercooling are other problems. Therefore, it seems encapsulation is an effective solution for the inherent problems of PCMs. Nanoencapsulated PCMs are very small bicomponent particles consisting of a core material, the PCM, and an outer shell or capsule wall. PCMs can absorb and release large amounts of heat.

In several years, many methods such as in situ polymerization,[15] coacervation,[16] and interfacial polymerization[17] have been used for the encapsulation of PCMs. Inherently, these methods usually produce capsules ranging larger than one micrometer. However, in some applications especially in latent functionally thermal fluids[18] or the spinning of fine fibers containing encapsulated PCMs in the textile industry, microencapsulated PCMs had not done well under their usage. The reason is that in thermal fluids, the large particles of microencapsulated PCMs cause the increase in a fluid's viscosity and often crush during pumping as well. In the textile industry, the use of microcapsules in a fine fiber matrix causes a decrease in the strength and tenacity of the produced fibers. Hence, it is indispensable to develop nanoencapsulated PCMs with smaller particles in comparison with microencapsulated ones.[19]

There exists several reports in the literature on microencapsulation of PMMA,[20−22] but because of the recent developments, miniemulsion polymerization has shown its viability in the preparation of nanocapsules both in fundamental and industrial research. One of the strength points of the miniemulsion process is the formation of polymeric nanocapsules consisting of polymers with encapsulated materials.[23,24] These structures are not often accessible using other types of heterophase polymerization techniques. There is limited precedence for producing nanoencapsulated PCMs by this technique. Landfester and co-workers[25]

Received: July 2, 2011
Revised: August 20, 2011
Published: September 02, 2011

first used the miniemulsion polymerization technique to elaborate nanocapsules by encapsulation of a liquid hydrocarbon core, and then several other groups adopted similar strategies.[26−28] Luo and Zhou[26] used the miniemulsion polymerization of styrene and methacrylic acid for the shell material and paraffin as the core. They studied some important factors such as the level and type of surfactant, level of hydrophilic comonomer, and the paraffin/monomer ratio. It was found that all above factors influence the morphology of nanocapsules. Fang et al.[19] prepared and characterized nanoencapsulated PCM with polystyrene as the shell and *n*-octadecane as the core by the ultrasonic-assisted miniemulsion polymerization. They showed that most of the produced nanocapsules were spherical and ranged from 100 to 123 nm in size. Park et al.[29] prepared polystyrene (PS) nanoparticles containing paraffin wax as the PCM by miniemulsion polymerization.

There are two approaches regarding the encapsulation of hydrophobic agents, specifically *n*-hexadecane in the literature. Some researchers consider it as a PCM and focus on its thermal properties and high thermal energy capability. Hence, their investigation is mainly based on thermal analysis techniques. In another point of view, these materials are taken into account as a hydrophobic agent, which are vital for the preparation of polymeric particles with controlled morphology and particle size, and thermal behavior is ignored.[28,30−34] Therefore, it seems necessary to have a combination of these concepts and bring thermal and morphological properties together.

With such an attitude, the encapsulation of *n*-hexadecane in polymethyl methacrylate as a model polymer for the preparation of PCM nanocapsules through miniemulsion polymerization has been studied extensively here, and several processing parameters such as the HD:MMA ratio, roll of cross-linking agent, and homogenization type were investigated. Also, the theoretical calculative method for prediction of PCM characteristics was developed. The experimental results beside the theoretical ones were exploited for the determination of the shell thickness in nanocapsules and the abundance of produced pure polymeric particles without PCM properties. These results also led us to determine the core content and encapsulation efficiency of the final PCM nanocapsules.

EXPERIMENTAL SECTION

Materials. Methyl methacrylate (MMA) was used as the monomer in the composition of the shell. Sodium dodecyl sulfate (SDS) and PEG (20) sorbitan monolaurate (Tween 20) were applied as surfactants. Benzoyl peroxide (BPO) was employed as a hyrophobic initiator. *n*-Hexadecane (HD) as a PCM and ethylene glycol dimethacrylate (EGDMA) as a cross-linking agent were used in the experiments. All above materials were purchased from Merck Chemical Co. except SDS (from Aldrich) and were used as received without further purification. Deionized water (DI) was consumed in all polymerization recipes. Commercial microcapsules (mPCM 18-D) were supplied from Microtek Co. (Dayton, OH, USA) and used for the shell thickness estimation and subsequent evaluation of pure polymeric particles.

Characterization. SONOPULS ultrasonic homogenizer (20 kHz ± 500 Hz Ultrasonic generator) Model HF-GM 2200 (BANDELIN electronic GmbH & Co. KG, Berlin, Germany) was used for miniemulsification, and the probe was a titanium microtip KE-76 with the diameter of 6 mm. Pre-emulsification was performed by a T25 digital ULTRA-TURRAX homogenizer that was equipped with a dispersing element, model S25N-25G (IKA Co. Germany). Differential scanning calorimetry (DSC) was performed by Polymer Laboratories Instruments Co. (USA), and all measurements were carried out under N_2 atmosphere at a heating and cooling rate of 10 °C/min, and the weight for each sample was about 5 mg. The heating scan was from −30 to 130 °C and, the cooling scan was performed in the above range too. Thermogravimetric analysis (TGA) was used for the investigation of thermal stability of the nanocapsules, and all experiments were performed at a heating rate of 20 °C min^{-1} in the temperature range of 25 to 600 °C under nitrogen atmosphere by TA Instruments Co. Model Q50 (USA). Transmission electron microscopy (TEM) was taken with a ZEISS 902A (Oberkochen, Germany) electron microscope operating at an acceleration voltage of 80 kV. The samples were diluted up to 20 times, mounted on 400-mesh carbon-coated grids, and left to dry for TEM analysis. Also, sample preparation for the determination of shell thickness was done by spray drying of latexes to obtain a fine powder. The powder was subsequently embedded in agar resin and cured at 60 °C for 2 h, after which it was washed with water. Then it was microtomed at ambient temperature by an Ultracut S (Leica, Vienna, Austria) ultramicrotome, equipped with a diamond knife, to produce slices with a thickness of 100 nm. These slices were placed on a copper grid for analyzing by TEM. In addition to TEM micrographs, the morphologies were also examined using scanning electron microscopy (SEM) with TESCAN Instruments Co. Model VEGA-II (Brno, Czech Republic). A drop of latex was placed on the sample holder and dried under freeze-drying. They were then put under vacuum, flushed with argon, evacuated, and sputter-coated with gold for SEM analysis. For observing the shell thickness by using SEM, the proper amount of microcapsule powder was mixed with a polyester thermoplastic adhesive (Phatilon H5) from Epurex films (GmbH & Co. KG, Bayer, Germany) and then placed in an aluminum mold and cured at room temperature to immobilize microcapsules in the polyester matrix. The molded sample was then microtomed and used for further investigation. Particle size analysis was carried out by using a dynamic light scattering (DLS) apparatus (Malvern instruments Co. UK), and all the samples were diluted to proper concentration before analysis. The solid contents were determined gravimetrically by drying a specified amount of latex.

Synthesis of the Nanoencapsulated PCMs. The basic recipe for all experiments is as follows and the differences for each set of experiments have been given in the corresponding tables. MMA and HD with desired amounts were mixed with the initiator and added to a solution of different amounts of surfactant(s) in 160 g of DI water with a predetermined 20 wt % solid content. After being pre-emulsified by a homogenizer at a rate of 11000 rpm for 15 min, miniemulsification was continued by ultrasonicating the mixture for 5 min at 75% amplitude. To avoid prepolymerization, the mixture was cooled in an ice-bath during sonication. The obtained miniemulsion was poured into a three-necked reactor equipped with a mechanical stirrer, condenser, and inlet for nitrogen gas. Before starting the reaction, the reactor was purged with nitrogen for 10 min to remove oxygen. The reaction was carried out for 5 h under a nitrogen atmosphere at 65 °C and stirred at 500 rpm. Finally, the prepared latex was cooled down to room temperature for further analysis. However, for removal of the adsorbed hexadecane on the surface of nanoparticles, the dried polymer was dispersed in *n*-hexane by using an ultrasonic bath, centrifuged, decanted, and dried at room temperature.

RESULTS AND DISCUSSION

Formation of nanocapsules containing PCMs or hydrophobe through miniemulsion polymerization is a challenging issue of polymer reaction engineering in dispersed media because several parameters have great influences on the properties of nanocapsules. Among them, HD:MMA ratios, the effect of the cross-linking agent, and homogenization recipe are studied here. In addition to the above parameters, the applied procedure greatly affects the hexadecane loading in the final particles.

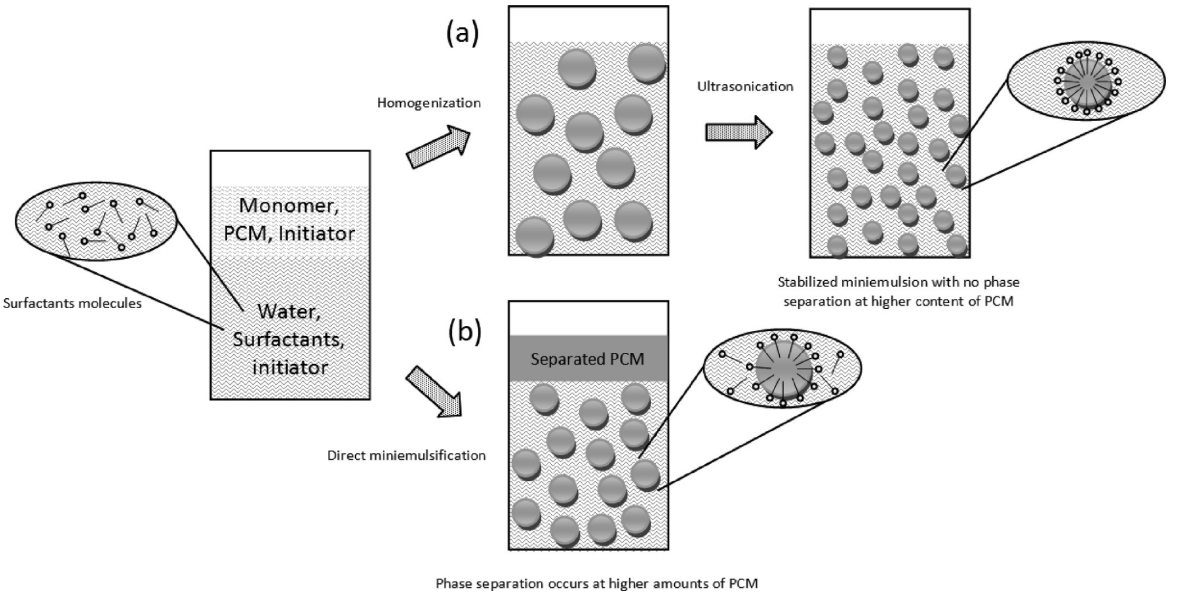

Figure 1. Schematic representation of the miniemulsification process (a) with pre-emulsification by using a homogenizer and (b) with direct ultrasonication and the absence of induced shear by the homogenizer.

Table 1. Preparation of Several PCMs at Different HD:MMA Weight Ratios[a]

sample	HD (g)	MMA (g)	EGDMA (g)	HD:MMA weight ratio	conv (%)
nPCM0	0.20	40.00		~0	90
nPCM1	10.00	30.00		1:3	82
nPCM2	16.00	24.00		2:3	90
nPCM3	20.00	20.00		3:3	95
nPCM4	24.00	16.00		3:2	90
nPCM5	30.00	10.00		3:1	87
nPCM6	32.00	8.00		4:1	
nPCM13	20.00	20.00	0.40	3:3	90
nPCM14	24.00	16.00	0.32	3:2	87
nPCM15	30.00	10.00	0.20	3:1	

[a] For all experiments, the concentration of BPO was kept constant at 25 mg of BPO/g of MMA. Deionized water (160 g), SDS (600 mg), and Tween 20 (in equal weight ratio) were used.

Ostwald ripening is a common phenomenon observed in miniemulsion polymerization. Because of the difference in osmotic pressure between small and large monomer droplets, monomer molecules in the smaller droplets are constrained to dissolve in water, diffuse through the aqueous phase, and then enter into the larger ones. As a consequence, larger monomer droplets grow up in size at the expense of the shrinkage of smaller ones, and finally, this diffusional degradation process will destabilize the miniemulsion. A hydrophobe such as HD or cetyl alcohol (CA) is often added into the recipe of miniemulsion polymerization in order to suppress the influence of Ostwald ripening, formation of monosize and stable monomer droplets, and retard diffusion of the monomer from small droplets to large ones.[35] In another viewpoint, higher content of HD would cause high latent heat and its viability for heat storage applications. Therefore, an increase in the HD:MMA ratio to some reasonable extent is a promising way to achieve a high heat energy storage density for those particles. The key point to suppress premature polymerization during ultrasonication is the placement of the reactor in an ice bath where HD solidifies and prevents the formation of stable minidroplets. Here, we found that homogenization by a high speed homogenizer before ultrasonication will result practically in an increase in the loading of PCM inside PMMA nanocapsules. The reason might be due to the increase in local heat around the dispersing element of the homogenizer, subsequent melting of HD, and formation of stabilized minidroplets. Figure 1 illustrates the schematic view of the miniemulsification process to achieve the production of stable PCM encapsulated latex particles. Some important parameters by using the above modified procedure will be studied in detail here.

Effect of HD:MMA Weight Ratio. Different weight ratios of *n*-hexadecane as the PCM to MMA were investigated in the first series of experiments. The basic recipe has been summarized in Table 1. Miniemulsions were prepared by mixing MMA and HD in the presence of an oil soluble initiator (BPO) and emulsifying the resulting mixture in an aqueous solution of equal amounts of SDS and Tween 20. MMA and HD are completely miscible, but phase separation occurs during the polymerization process due to the immiscibility of HD and PMMA. Phase separation was observed for nPCM6, and two phases were completely separated at the end of polymerization. Conversions were determined at the end of polymerization and based on gravimetric analysis. nPCM0 was considered as the blank sample, and the added HD in the recipe was used in order to suppress Ostwald ripening during miniemulsion polymerization. These series of experiments illustrated that the highest encapsulation efficiency in spherical particles was obtained at a 3:1 weight ratio of HD:MMA, and at higher ratios, phase separation occurred at the end of polymerization due to the instability of the system.

Size Distribution and Morphological Studies of the Nanocapsules. Dynamic light scattering (DLS) analysis was used to investigate particle size and their distribution in the latexes, and the results showed that nanocapsules were ranging from

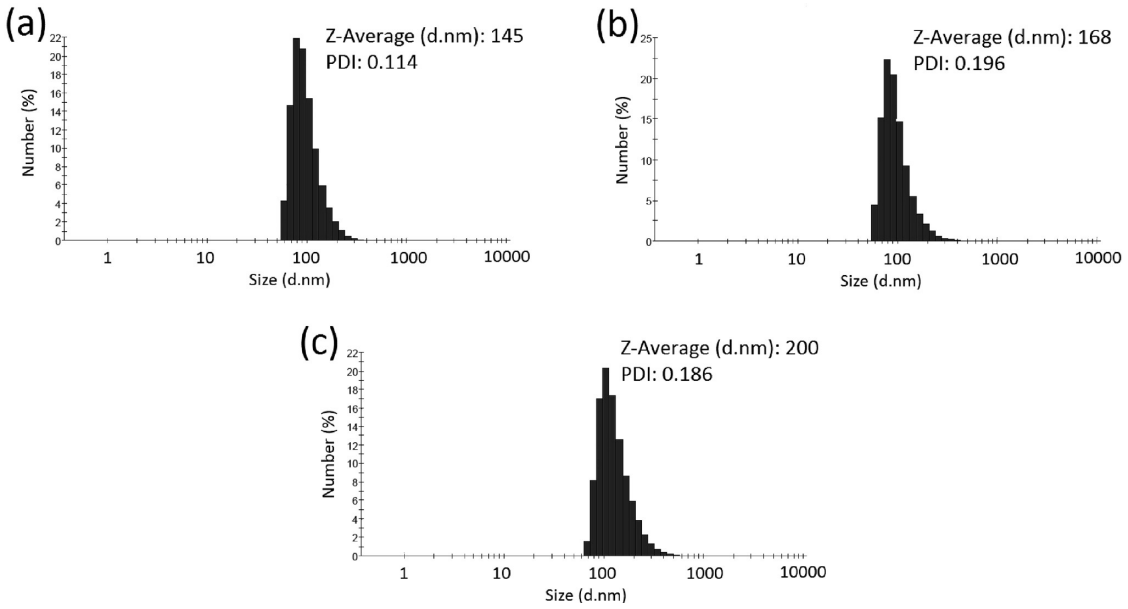

Figure 2. Particle size distribution of nanocapsules for nPCM0 (a), nPCM3 (b), and nPCM5 (c) with 0, 3:3, and 3:1 weight ratios of HD:MMA, respectively.

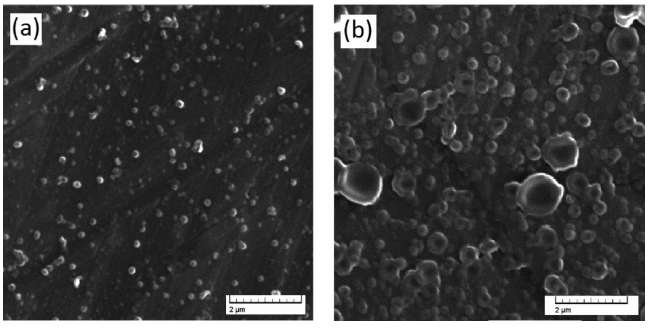

Figure 3. SEM micrographs of nPCM0 (a) and nPCM5 (b) with 0 and 3:1 weight ratios of HD:MMA, respectively.

50 to 600 nm. Figure 2 reveals size distribution curves for the blank sample (nPCM0), nPCM3, and nPCM5. It was observed that by increasing the amount of HD from 0.2 g in nPCM0 to 30 g in nPCM5, the mean diameter of the nanoparticles increased from 145 nm (nPCM0) to 200 nm (nPCM5). It is believed that by increasing the HD amount and keeping the surfactants at a constant level, contribution of the surfactant molecules per particle is decreased, and the size of the stabilized droplets is increased consequently.

Scanning electron microscopy (SEM) results for some typical samples (nPCM0 and nPCM5) have been given in Figure 3. In these micrographs, spherical nanocapsules with smooth surfaces are clearly observable, and their sizes are in good agreement with DLS results.

Transmission electron microscopy (TEM) of the latex particles have been shown in Figure 4. For nPCM0, spherical particles are found, and by increasing HD content in nPCM5, core−shell morphology is clearly observed and formation of nanocapsules is confirmed (Figure 4b). The dark layer reveals the PMMA shell, and the light core is attributed to the encapsulated HD inside the nPCM5 nanocapsules.

Phase Change Characteristics of Nanocapsules. The phase change properties of nanocapsules can be studied by using some

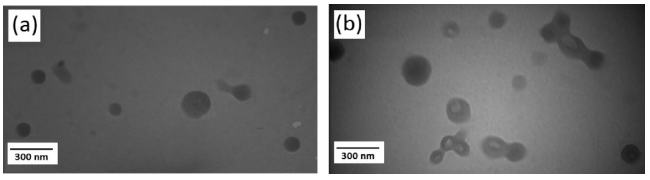

Figure 4. TEM micrographs of nPCM0 (a) and nPCM5 (b) with 0 and 3:1 weight ratios of HD:MMA, respectively.

important equations to describe the characteristics of produced PCM particles. The theoretical core content (C_t) can be considered as the weight ratio of HD (W_{HD}) to the total amount of HD and monomer (W_m) as shown below (eq 1):

$$C_t = \left(\frac{W_{HD}}{W_{HD} + W_m}\right) \times 100 \quad (1)$$

The experimental core content (C_e) in the dried latex is based on the enthalpies obtained from DSC thermograms multiplied by conversion (Conv.) according to eq 2.

$$C_e = \left(\frac{\Delta H_{m,e}}{\Delta H_{m,c}}\right) \times \text{Conv.} \quad (2)$$

where, $\Delta H_{m,e}$ is the recorded heat of melting for the dried PCM nanocapsules, relating to the encapsulated HD, and $\Delta H_{m,c}$ is the heat of melting of pure *n*-hexadecane (equal to 213.2 J/g). However, the actual core content of nanocapsules (C'_e) could be defined as (eq 3)

$$C'_e = \left(\frac{\Delta H'_{m,e}}{\Delta H_{m,c}}\right) \times \text{Conv.} \quad (3)$$

where, $\Delta H'_{m,e}$ is the recorded heat of melting for the washed and dried particles with *n*-hexane as a solvent of HD for removal of any probable adsorbed HD on the surface of particles. Notably, adsorption of HD on the surface particles or nanocapsules is

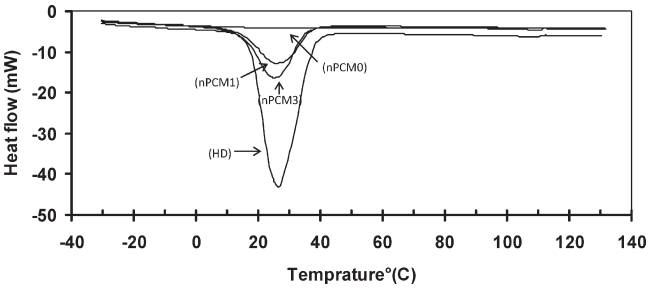

Figure 5. DSC thermograms for PMMA polymer particles (nPCM0), pure *n*-hexadecane (HD) and some prepared nanocapsules at different HD:MMA ratios.

Table 2. Thermal Parameters and Corresponding Calculated Encapsulation Characteristics for the Different Prepared PCM Nanocapsules

sample	$\Delta H_{m,e}$ (J/g)	$\Delta H'_{m,e}$ (J/g)	C_t (%)	C_e (%)	C'_e (%)	S (%)	E (%)
nPCM0			0.00				
nPCM1	73.95	67.42	25.00	28.44	25.91	8.89	84.98
nPCM2	74.50	67.73	40.00	31.44	28.56	9.16	64.26
nPCM3	75.27	68.07	50.00	33.50	30.30	9.55	57.27
nPCM4	82.14	74.06	60.00	34.64	31.23	9.84	46.85
nPCM5	96.76	86.27	75.00	39.45	35.17	10.85	41.74
Pure HD	213.20						

inevitable, and this will cause some deviation in the calculations based on thermal studies. For this reason, it will be able to evaluate the fraction of surface absorbed HD on the particles (S) as shown below (eq 4):

$$S = \left(1 - \frac{C'_e}{C_e}\right) \times 100 \quad (4)$$

The encapsulation efficiency (E) is measured by the ratio of the actual core content of the nanocapsules to the theoretical one multiplied by the conversion for each sample (eq 5).

$$E = \left(\frac{C'_e}{C_t}\right) \times \text{Conv.} \quad (5)$$

Figure 5 reveals DSC thermograms of some typical samples at various HD:MMA ratios and also pure HD. All measurements were carried out under N_2 atmosphere at a heating rate of 10 °C/min, and the amount of each sample was about 5 mg, and heating scans were between −30 to 130 °C. Cooling scans were performed from 130 to −30 °C with a similar heating rate, and the crystallization temperatures were found to be almost 10 °C below the observed melting point. The difference between the enthalpy of melting and crystallization was negligible, and the enthalpy of melting was considered for our further calculations. It is notable that by increasing the HD content in the recipes, the amount of melting enthalpy increased due to the higher contribution of HD during the encapsulation process.

The obtained numerical results from the DSC thermograms, based on eqs 1−5, have been summarized in Table 2. According to eq 1, C_t has direct relationship with W_{HD}, but there is a limitation in the increasing core content and encapsulation efficiency due to the processing parameters. These parameters would be stabilization in the system, nature of monomers, and also cross-linking density of the polymeric shell. This was experienced in our system in which a higher level of HD content resulted in phase separation at the end of polymerization (nPCM6). Equation 2 describes the amount of HD in the dried latex (C_e) that is a summation of the encapsulated HD and probable surface adsorbed HD. By increasing the amount of C_t, C_e increases due to the higher contribution of HD in the dried latex (Table 2). To measure the surface adsorbed HD, 2 g of the dried latex was ground, powdered, and dispersed in 5 mL of *n*-hexane as a solvent of HD. Then, it was sonicated in an ultrasonic bath for one minute, and the mixture was centrifuged at the rate of 2000 rpm for 2 min. Finally, the obtained precipitate was decanted, dried at room temperature, and used for the determination of $\Delta H'_{m,e}$.

It is worth mentioning that by increasing C_t, C'_e increases as well as S but not with the same rate. The results for the calculated encapsulation efficiency (E) depict that higher E values are obtained at lower HD:MMA ratios, and by increasing this ratio, the probability of the encapsulation of HD is decreased until phase separation occurs in nPCM6. By increasing the HD:MMA ratio, it is expectable that shell thickness decreases, and the diffusion of HD from nanocapsules to the continuous phase will predominate and result in the phase separation.

This information has been plotted in Figure 6 to give a better illustration on the variation of those parameters with HD:MMA ratio in the recipes.

Another important deduction from the above quantitative parameters is to elucidate the thermodynamic stability and capacity of the monomer droplets to reside in the added PCM. The comparison between C_t and C'_e in our experiments depicts that there should be an optimum for HD for effective encapsulation. At higher amounts of HD, no effective encapsulation occurs, and the extra HD is just adsorbed on the surface of the capsules. These have been plotted in Figure 7 to demonstrate the divergence between C_t and C'_e at higher levels of HD. This continues until the extra amount of HD can not be stabilized on the surface of the capsules, and an entire phase separation is observed, which was found for nPCM6.

Thermal Stability of Nanocapsules. Thermal stability is an important factor in the assessment of encapsulated PCMs in their application for heat energy storage or thermal regulation. Thermal stability of the prepared nanocapsules was investigated by means of TGA. TGA thermograms of nanocapsules at different ratios of HD:MMA have been given in Figure 8, and quantitative results have been plotted in Figure 9, representing definite weight losses at various temperatures. It is observable that the weight loss profiles of all nanocapsules containing HD are quite similar and that their thermal decompositions perform through a two-step degradation process between 25−600 °C. The similarity in the temperatures for occurrence of weight losses of 5 wt % (T_{d5}) and 20 wt % (T_{d20}) for pure HD and the prepared nanocapsules (except for nPCM0) depicts that they obey the same pattern in thermal degradation due to the presence of loosely bound subsurface HD in the nanocapsules (Figure 9).

PMMA (nPCM0) shows a very slight weight loss below 150 °C, and this could be attributed to the leakage of HD, which is very close to the particle's surface. The role of shell thickness is more sensed above 170 °C in which thermal degradation of PMMA starts. Pure HD completely disappears below 200 °C, and the intermediate stability of nanocapsules (between two limits of HD and nPCM0) reveals the characteristics of a polymeric shell, its thickness, and resistance against leakage of HD. It is expected that by decreasing the HD:MMA ratio, shell thickness

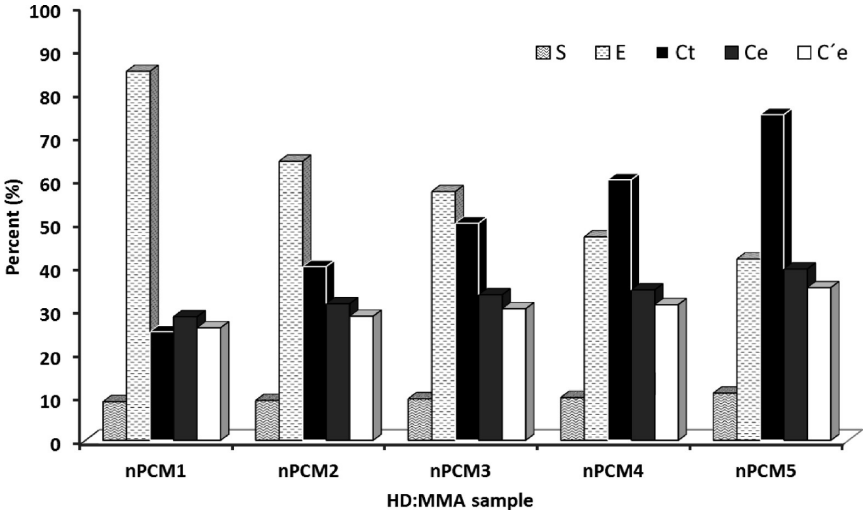

Figure 6. Variation of C_t and thermal characteristics for the prepared PCM nanocapsules with different HD:MMA weight ratios.

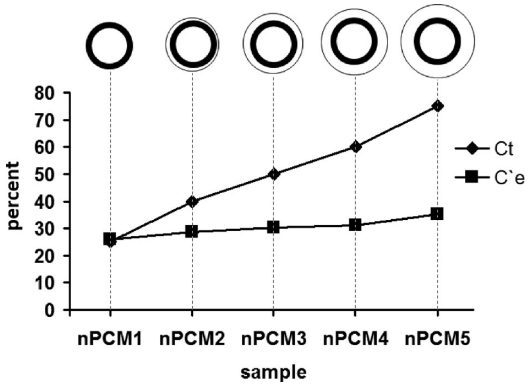

Figure 7. Divergence between C_t and C'_e for the prepared PCM nanocapsules with different HD:MMA weight ratios.

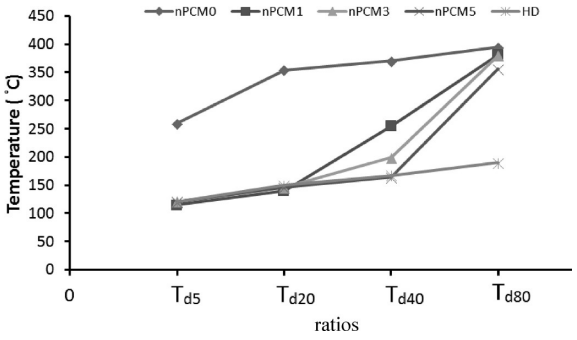

Figure 9. Definite weight losses at various temperatures for pure HD and the prepared PCM nanocapsules at different HD:MMA ratios. T_{d40} and T_{d80} exhibit the required temperature for weight losses of 40 and 80 wt %, respectively.

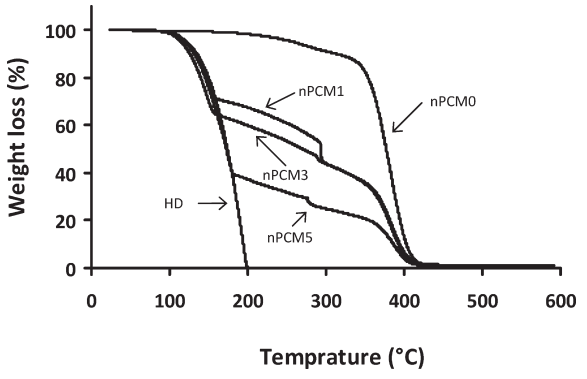

Figure 8. TGA thermograms of pure HD and prepared nanocapsules at different HD:MMA ratios.

increases, and the resulting nanocapsules exhibit more thermal stability and less tendency toward releasing the engulfed HD. Verification of the shell thickness in the prepared PCM nanocapsules will be elaborated in the upcoming sections.

Effect of Cross-Linking of the Shell. By using EGDMA as a cross-linking agent, nanocapsules with higher dimensional and thermal stability of the shell can be obtained. Three samples (nPCM13-15) were prepared in this study (Table 1) and nPCM15 was not considered for further investigations due to the high coagulation amount. Typical TGA thermograms of the prepared nanocapsules under different HD:MMA ratios without any EGDMA (nPCM3 and nPCM4) and in the presence of EGDMA (nPCM13 and nPCM14) have been shown in Figure 10.

It is obvious that the initial thermal stability increases for nPCM13 and nPCM14 relative to nPCM3 and nPCM4, respectively. Notably, nPCM3 loses more than 30 wt % at 180 °C, and this is just 10% for nPCM13. Similar results could be found for nPCM14, revealing higher stability of the shell during network formation. It is also interesting that the two-step degradation is repeated for the cross-linked samples and that they obey the same thermal degradation profile as the noncross-linked ones. DSC studies on the cross-linked nanocapsules were carried out, and the obtained thermal parameters and encapsulation parameters have been summarized in Table 3. The comparison between these parameters represents a remarkable development in nPCM13 and nPCM14 with respect to uncured ones. For instance, the increase in C'_e and E was about 60% and 55%, respectively, for nPCM14 relative to nPCM4. The results show that cross-linking

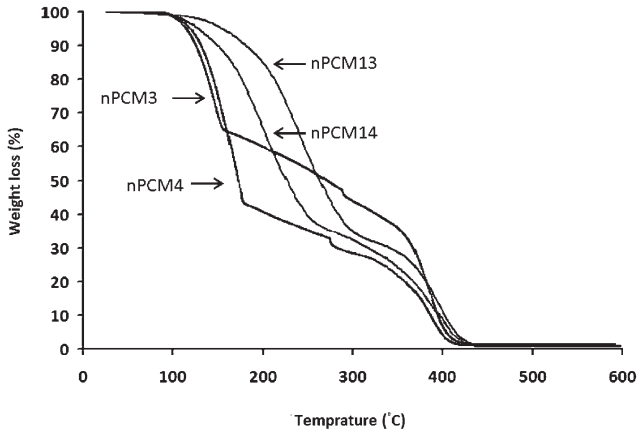

Figure 10. TGA thermograms of the prepared nanocapsules (nPCM3, nPCM4) and corresponding cross-linked shell (nPCM13, nPCM14) at different HD:MMA ratios.

Table 3. Thermal Parameters and Corresponding Calculated Encapsulation Characteristics for the Cross-Linked Nanocapsules

sample	$\Delta H_{m,e}$ (J/g)	$\Delta H'_{m,e}$ (J/g)	C_t (%)	C_e (%)	C'_e (%)	S (%)	E (%)
nPCM13	98.00	95.46	50.00	41.36	40.29	2.59	72.52
nPCM14	130.96	122.64	60.00	53.44	50.05	6.34	72.57

of the shell caused a significant decrease in the surface adsorbed HD (S) too.

It seems that cross-linking of the polymeric shell during the encapsulation phenomenon, which occurs inside of droplets, will reduce chain mobility. This interruption postpones the migration of polymeric chains toward the shell and consequently the reduction in potential capacity of the nanocapsules. In other words, phase separation will occur predominantly at higher HD:MMA ratios, at the end of the polymerization reaction, which was found for nPCM15.

Measurement of Shell Thickness and Abundance of Pure Polymeric Particles in Nanocapsules. Release or leakage of the core material through the shell is mainly controlled by the thickness of the shell and its porosity. Here, we will discuss spherical core−shell micro/nanocapsules, measurement of the shell thicknesses of the capsules, and estimation of the abundance of pure polymeric particles without any HD contamination. For the above evaluations, a new approach by combination of DSC, DLS, and electron microscopy (SEM and TEM) analyses has been developed here. The experimental core content in the dried sample (C'_e) is expressed based on the enthalpies obtained from DSC thermograms (eq 3). The key point in this step is to assume conversion equal to 100% for the dried latexes. This assumption is valid for any dried capsule; this is studied individually, and its actual core content can be considered independent of the polymerization process.

Therefore, the ratio of the weight fractions of the shell material (W_s) to that of the core material (W_c) could be defined as (eq 6)

$$\frac{W_s}{W_c} = \frac{1 - C'_e}{C'_e} \tag{6}$$

where $W_s + W_c = 1$.

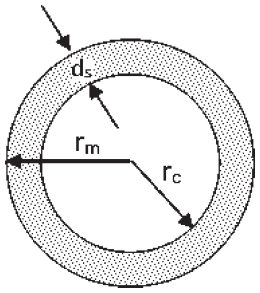

Figure 11. Schematic representation of a cross-section in an ideal capsule ($d_s = r_m - r_c$).

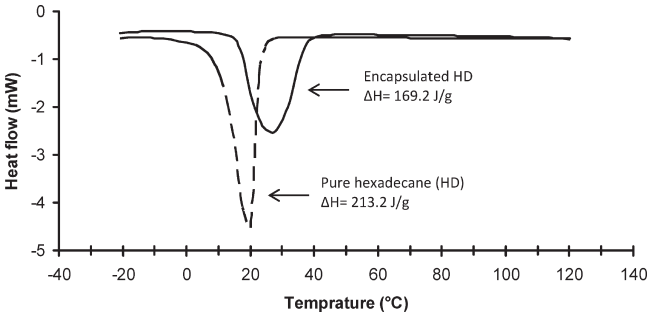

Figure 12. DSC thermograms of pure hexadecane and mPCM-18D microcapsules.

Figure 11 represents the cross-section of an ideal capsule in which d_s is the shell thickness, and r_c and r_m show the internal and external radii of this capsule, respectively. It is possible to establish the relationship between densities of the polymeric shell (ρ_s) and core content (ρ_c), r_m, and r_c, and also W_s and W_c in eq 7.[36]

$$\frac{W_s}{W_c} = \frac{\rho_s}{\rho_c} \times \frac{V_s}{V_c} = \frac{\rho_s}{\rho_c} \times \frac{(4/3)\pi (r_m^3 - r_c^3)}{(4/3)\pi r_c^3} \tag{7}$$

where V_s and V_c are the occupied volume by the shell and core, respectively.

Thus d_s is obtained through eq 8 by a simple rearrangement of eq 7.

$$d_s = r_m \times \left[1 - \left(\frac{W_s \rho_c}{W_c \rho_s} + 1\right)^{-1/3}\right] \tag{8}$$

Equation 8 is an ideal one and is correct in the case that nanocapsules are monosize, but there is usually a particle size distribution for the nanocapsules (with different radius). The corrected equation for describing the system could be considered as follows (eq 9):

$$\frac{W_s}{W_c} = \sum_{i=1}^{n} f_i \frac{w_{s_i}}{w_{c_i}} = \frac{\rho_s}{\rho_c} \times \sum_{i=1}^{n} f_i \left[\left(\frac{r_{m_i}}{r_{c_i}}\right)^3 - 1\right] \text{ and } \sum_{i=1}^{n} f_i = 1 \tag{9}$$

where f_i is the volume fraction of nanocapsules with overall number of n and the same size, r_{m_i} and r_{c_i} represent the radii of each volume fraction of nanocapsules (obtained from DLS), and

dx.doi.org/10.1021/ma201509d |*Macromolecules* 2011, 44, 7405–7414

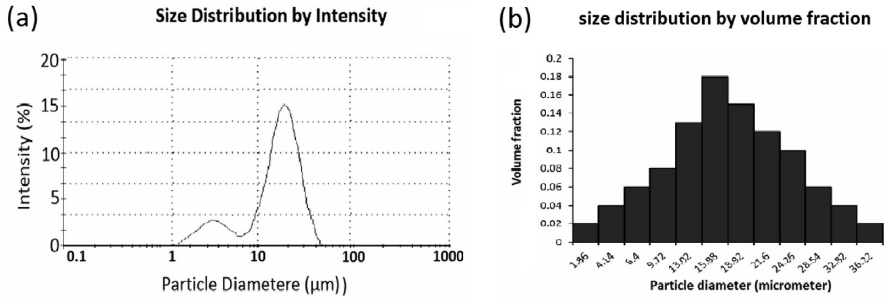

Figure 13. Particle size distribution for mPCM18-D standard microcapsules.

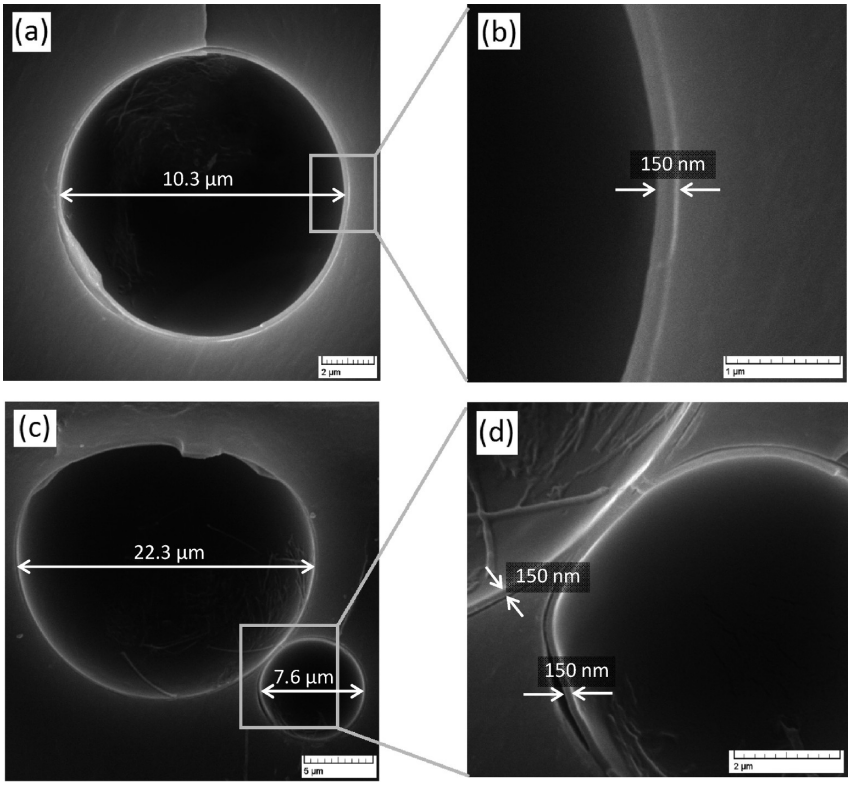

Figure 14. SEM micrograph of the cross-section of microtomed mPCM18-D microcapsules with lighter domains as an indication of the shell thickness.

w_{s_i}/w_{c_i} shows the weight ratio of each fraction. In other words, this ratio can be related to the shell thickness according to eq10.

$$\frac{W_s}{W_c} = \sum_{i=1}^{n} f_i \frac{w_{s_i}}{w_{c_i}} = \frac{\rho_s}{\rho_c} \times \sum_{i=1}^{n} f_i \left[\left(\frac{r_{m_i}}{r_{m_i} - d_s} \right)^3 - 1 \right] \qquad (10)$$

The above equation is valid while considering two assumptions: (i) all prepared capsules should be spherical, and this can be confirmed through morphological studies; (ii) the shell thickness for all capsules is constant and independent of the particle size. W_s and W_c are obtained from DSC, and r_{m_i} is extracted from DLS. Hence, d_s could be calculated from eq 10.

To evaluate the validity of calculated d_s, it is necessary to compare it with the experimental one (d'_s). As a consequence, one of the parameters that make deviation between d_s and d'_s is the probability of formation of pure polymeric particles that is unavoidable. These particles do not carry any HD and cannot participate in the phase change behaviors of the resulting product.

It is believed that in an ideal miniemulsion polymerization, all minidroplets include a hydrophobic agent (e.g., HD) with the same concentration, and there is no possibility of hydrophobe migration through the continuous phase. Therefore, the existence of pure polymeric particles (without any HD) can give an indication of the drift from miniemulsion polymerization. This drift reveals the probable polymerization of monomers in the continuous phase via homogeneous nucleation. As a consequence, measurement of existing pure polymeric particles and their abundance relative to the prepared micro/nanocapsules will forward us to the extent of driftness from the miniemulsion polymerization mechanism. This parameter is extensively discussed here as the result of the encapsulation process. The probability of existence of pure polymeric particles is more sensed here as MMA has a relative solubility in water of about 0.15 mol/L.[25]

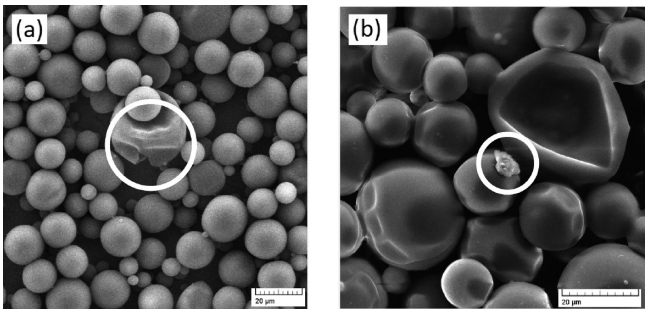

Figure 15. SEM micrographs of mPCM 18-D microcapsules containing some pure polymeric fractions without any HD.

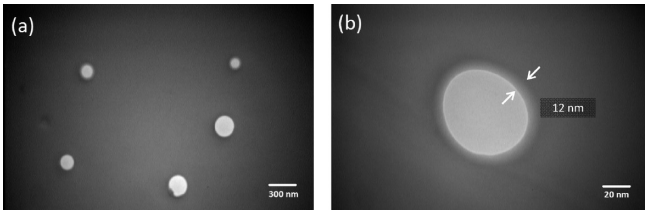

Figure 16. TEM micrographs of ultramicrtommed nPCM3 nanocapsules at different magnifications.

Direct determination of the weight fraction of the incorporated polymer in capsules (W'_s) can be achieved by measurement of d'_s by using microscopy analysis and replacing it in eq 10. Therefore, the weight fraction of pure polymeric particles (W_{PP}) could be obtained from $W_s - W'_s$.

To confirm these calculations, a commercial PCM microcapsule (mPCM18-D) from Microtek Co. (Dayton, OH, USA) was supplied, and the above analyses were performed for that sample typically. DSC analyses besides the pure HD one has been given in Figure 12 comparatively for the determination of W_s and W_c by using eq 3 and eq 6. Hence, C'_e and W_s/W_c were found to be 79.36% and 0.26, respectively for mPCM18-D.

Dynamic light scattering analysis was used to investigate particle size distribution and determination of abundance of each fraction with equal radius (r_{m_i}). It is notable that those fractions with similar r_{m_i} have the same w_{s_i}/w_{c_i}. Figure 13a shows the particle size distribution for mPCM18-D, and it has been fractionated due to the volume fractions of definite segments in Figure 13b. The obtained data from DLS and DSC led us to the shell thickness of 155 nm for nPCM-18D.

The comparison between the above calculated shell thickness (d_s) and the actual one (d'_s) from SEM analysis (Figure 14) will give an estimation of the extent of the actual weight fraction of a polymer (W'_s) containing HD in the resulting capsules.

It is obvious that shell thickness for the microcapsules with different sizes (Figure 14a,c) are the same and about 150 nm (Figure 14b,d) with reasonable approximation. Notably, this thickness is independent of the size of capsules in accordance with our assumption for eq 10.

The existence of pure polymeric fractions as the reason for the difference between d_s and d'_s has been pointed out in SEM micrographs of mPCM18-D in Figure 15.

On the basis of the above explanations, d_s and d'_s were calculated for nPCM1, nPCM3, and nPCM5. Figure 16 represents TEM micrographs of ultramicrotomed nanocapsules in agar resin at different magnifications for nPCM3, typically with an actual shell thickness (d'_s) of about 12 nm and d_s of about 14 nm. The actual shell thickness was averaging of at least 50 nanocapsules in this analysis.

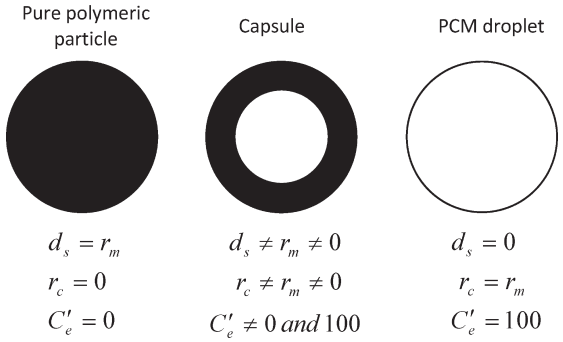

Figure 17. Schematic correlation between d_s, r_m, and C'_e.

Table 4. Some Comparative Calculated Characteristics for Different Samples

sample	ρ_s (g/cm^3)	d_s (nm)	d'_s (nm)	W_{PP}	W'_s	void fraction (%)
mPCM18-D	1.50	155	150	0.01	0.20	92.3
nPCM1	1.18	14	12	0.17	0.49	68.5
nPCM3	1.18	14	12	0.16	0.48	68.5
nPCM5	1.18	13	11	0.12	0.50	76.5

To have an animated representation of the formation of capsules, three situations could be considered (Figure 17). Two of them are extreme conditions in which $d_s = 0$ and $d_s = r_m$. In the middle of these limits, there will be the possibility of the encapsulation of the PCM inside the polymeric shell with different shell thicknesses.

These results for the known sample (mPCM18-D) together with the prepared ones through miniemulsion polymerization have been summarized in Table 4.

The comparison between obtained W_{PP} for the samples depicts that mPCM18-D has the highest W'_s and lowest W_{PP}. In other words, this sample has had maximum microcapsules, including HD, with a higher contribution level of polymeric phase for the encapsulation phenomenon. This has reduced for the products from the nPCM series, regarding the fact that at higher HD:MMA ratios, the probability of encapsulation increases to some extent, and W_{PP} is decreased, but as a penalty of the decrease in efficiency and a sharp drop in thermal stability.

CONCLUSIONS

Because of a considerable difference in polarity of *n*-hexadecane and PMMA, the system is well-suited for the preparation of nanocapsules containing HD as a PCM. It was shown that some parameters such as HD:MMA ratio and using EGDMA as a cross-linking agent have great influences on size, morphology, thermal stability, and thermal storage behavior of the produced nanocapsules. A new approach using DSC, DLS, and microscopy was developed to estimate shell thickness (d_s), extent of contribution of the polymeric shell in the formation of nanocapsules (W'_s), and the weight fraction of pure polymeric particles (W_{PP}). The most important results during this study are as follows:

(1) It is possible to increase the HD:MMA ratio up to 3:1, but it causes a sharp drop in efficiency of the encapsulation process (E).
(2) At higher amounts of HD, the divergence between C_t and C'_e is increased, and the extra amount of HD is adsorbed on the surface of the resulting capsules.
(3) EGDMA increases encapsulation efficiency and actual core content of nanocapsules by 60% and 55%, respectively. This is due to the improvement in thermal stability and reduction in porosity of the nanocapsule shell because of the enhancement in the corresponding dimensional stability.
(4) Shell thickness and weight ratio of pure polymeric particles were estimated. This was used to evaluate the probability of formation of pure polymeric particles. The results revealed a higher W_{PP}, which would be due to the homogeneous nucleation through miniemulsion polymerization.
(5) Void fraction was calculated for the samples from miniemulsion polymerization, and it was found that this parameter has a direct relationship with the HD:MMA ratio.

AUTHOR INFORMATION

Corresponding Author

*Tel: +9821 4458 0000. Fax: +9821 4458 0023. E-mail: a.mahdavian@ippi.ac.ir.

ACKNOWLEDGMENT

We would like to express our gratitude to the Iran Polymer and Petrochemical Institute (IPPI) for the financial support with Grant No. 24752105. Also, the fruitful collaboration of M. Motamedi and J. Nadali is greatly acknowledged.

APPENDIX

C_t	theoretical core content
W_{HD}	weight of HD
W_m	weight of monomer
C_e	experimental core content
$\Delta H_{m,e}$	heat of melting for the dried PCM nanocapsules
$\Delta H_{m,p}$	heat of melting of the pure HD
C'_e	actual core content of nanocapsules
$\Delta H'_{m,e}$	heat of melting for the washed and dried particles
S	fraction of adsorbed HD
E	encapsulation efficiency
W_s	weight fraction of the shell
W_c	weight fraction of the core
d_s	calculated shell thickness
r_m	external radius of the capsules
r_c	internal radius of the capsules
ρ_s	density of polymeric shell
ρ_c	density of liquid core (HD)
V_s	occupied volume by the shell
V_c	occupied volume by the core
f_i	volume fraction of capsules
r_{m_i}	external radius of the capsules for fraction i
r_{c_i}	internal radius of the capsules for fraction i
d'_s	actual shell thickness
W_{PP}	weight fraction of existing pure polymeric particles
W'_s	weight fraction of polymer containing HD
w_{s_i}/w_{c_i}	weight ratio of polymeric shell to the encapsulated one for fraction i

REFERENCES

(1) Dergunov, S. A.; Kesterson, K.; Li, W.; Wang, Z.; Pinkhassik, E. *Macromolecules* **2010**, *43*, 7785–7792.
(2) Feng, X.; Jin, Z. *Macromolecules* **2009**, *42*, 569–572.
(3) Li, W.; Matyjaszewski, K.; Albrecht, K.; Miler, M. *Macromolecules* **2009**, *42*, 8228–8233.
(4) Li, W.; Yoon, J. A.; Matyjaszewski, K. *J. Am. Chem. Soc.* **2010**, *132*, 7823–7825.
(5) Rosenbauer, E.; Landfester, K.; Musyanovych, A. *Langmuir* **2009**, *25*, 12084–12091.
(6) Zhihai, C.; Ziener, U.; Landfester, K. *Macromolecules* **2010**, *43*, 6353–6360.
(7) Menyah, K.; Wolde-Rufael, Y. *Energy Policy* **2010**, *38*, 2911–2915.
(8) Scarpa, R.; Willis, K. *Energy Econ.* **2010**, *32*, 129–136.
(9) Rady, M. A.; Arquis, E.; Le Bot, C. *Int. J. Energy Res.* **2010**, *34*, 333–344.
(10) Takahiro, N.; Noriyuki, O.; Tomohiro, A. *Mater. Chem. Phys.* **2009**, *115*, 846–850.
(11) Kenisarin, M. M. *Renewable Sustainable Energy Rev.* **2010**, *14*, 955–970.
(12) Pasupathy, A.; Velraj, R. *Energy Buildings* **2008**, *40*, 193–203.
(13) Diaconu, B. M.; Varga, S.; Oliveira, A. C. *Appl. Energy* **2010**, *87*, 620–628.
(14) Sánchez, P.; Sánchez-Fernandez, V. M.; Romero, A.; Rodríguez, J.; Sánchez-Silva, L. *Thermochim. Acta* **2010**, *498*, 16–21.
(15) Alkan, C.; Sarı, A.; Karaipekli, A.; Uzun, O. *Sol. Energy Mater. Sol. Cells* **2009**, *93*, 143–147.
(16) Bayés-García, L.; Ventolà, L.; Cordobilla, R.; Benages, R. C., T.; Cuevas-Diarte, M. A. *Sol. Energy Mater. Sol. Cells* **2010**, *94*, 1235–1240.
(17) Su, J. F.; Wang, L. X.; Ren, L. *Colloid Surf., A* **2007**, *299*, 268–275.
(18) Fang, Y.; Kuang, S.; Gao, X.; Zhang, Z. *J. Phys. D: Appl. Phys.* **2009**, *42*, 035407.
(19) Fang, Y.; Kuang, S.; Gao, X.; Zhang, Z. *Energy Convers. Manage.* **2008**, *49*, 3704–3707.
(20) Sennur, A.; Cemil, A.; Fethiye, G. *Thermochim. Acta* **2011**, *518*, 1–8.
(21) Xiaolin, W.; Yihai, W.; Pengli, Z.; Rong, S.; Shuhui, Y.; Ruxu, D. *Matter. Lett.* **2011**, *65*, 705–707.
(22) Ahmet, S.; Cemil, A.; Karaipekli, A. *Appl. Energy* **2010**, *87*, 1529–1534.
(23) Mahdavian, A. R.; Ashjari, M.; Salehi-Mobarakeh, H. *J. Appl. Polym. Sci.* **2008**, *110*, 1242–1249.
(24) Mahdavian, A. R.; Sehri, Y.; Salehi-Mobarakeh, H. *Eur. Polym. J.* **2008**, 2482–2488.
(25) Tiarks, F.; Landfester, K.; Antonieti, M. *Langmuir* **2001**, *17*, 908–918.
(26) Luo, Y. W.; Zhou, X. D. *J. Polym. Sci., Part A: Polym. Chem.* **2004**, *42*, 2145–2154.
(27) Ni, K. F.; Shan, G. R.; Weng, Z. X. *Macromolecules* **2006**, *39*, 2529–2535.
(28) van Zyl, A. J. P.; Sanderson, R. D.; Wet-Roos, D.; Klumperman, B. *Macromolecules* **2003**, *36*, 8621–8629.
(29) Park, S. J.; Kim, K. S.; Hong, S. K. *Polymer (Korea)* **2005**, *29*, 8–13.
(30) Cao, Z. H.; Shan, G. R. *J. Polym. Sci., Part A: Polym. Chem.* **2009**, *47*, 1522–1534.
(31) Cao, Z. H.; Shan, G. R.; Sheibat-Othman, N.; Putaux, J. L.; Bourgeat-Lami, E. *J. Polym. Sci., Part A: Polym. Chem.* **2010**, *48*, 593–603.
(32) Chen, Y. C.; Dimonie, V.; Elaasser, M. S. *J. Appl. Polym. Sci.* **1991**, *42*, 1049–1063.
(33) McDonald, C. J.; Bouck, K. J.; Chaput, A. B.; Stevens, C. J. *Macromolecules* **2000**, *33*, 1593–1605.
(34) McDonald, C. J.; Devon, M. *J. Adv. Colloid Interface Sci.* **2002**, *99*, 181–213.
(35) Chern, C. S.; Chen, T. J. *Colloids Surf., A* **1998**, *38*, 65–74.
(36) Ghosh, S. K. In *Functional Coatings by Polymer Microencapsulation*; Wiley: Weinhem, Germany, 2006.